

Analysis and Modeling of Airgap & Zigzag Leakage Fluxes in a Surface-Mounted-PM Machine

Ronghai Qu, Student Member, IEEE and Thomas A. Lipo, Fellow, IEEE

Department of Electrical and Computer Engineering

University of Wisconsin - Madison

Madison, WI, USA

E-mail: ronghaiqu@ieee.org, and lipo@engr.wisc.edu

Abstract – In this paper the magnetic characteristics of surface-mounted permanent magnet machines are analyzed and modeled. The airgap and zigzag leakage fluxes are analytically expressed in terms of the magnetic material properties and the motor dimensions. Both factors are essential quantities for the accurate prediction of the flux distribution within the machine and of the machine torque. Therefore, they are desired for the purpose of machine design and optimization.

In order to evaluate the validity of the proposed models, the Finite Element Method (FEM) analysis is used. The results show that the errors between the FEM results and analytical predictions are less than 1% for both the airgap and zigzag leakage fluxes. This accuracy is also proven by the prototype measurements.

Keywords – Airgap leakage flux, zigzag leakage flux, PM machine, PM machine design

I. INTRODUCTION

Accompanied by the fast development of Permanent Magnet (PM) materials and the availability of modern power electronics, PM machine topologies have evolved quite quickly [1-3]. They have a wide variety of applications in the area of variable speed drives, servo drives, appliance and industrial automation. Therefore, design work on PM machines has becoming increasingly important.

It is well known that leakage flux has a substantial effect on the air gap fluxes interacting with the armature current to produce torque. It is an essential quantity for the accurate prediction of machine torque and the average flux densities within the air gap and the magnet. Therefore, it is desirable to analytically express the leakage flux factor in terms of the magnetic material properties and the machine dimensions. Although one paper [4] covering the airgap leakage flux calculation in a buried PM machine was published that predicts errors of 2%, one for surface-mounted PM machines is still not currently available. This kind model is highly desired and good accuracy is required for the purpose of machine design and optimization. To derive this model is one of two focuses in this paper.

In addition to the air gap leakage flux, zigzag leakage flux is another main part of the leakage flux. The zigzag leakage can be composed of three portions: one part of the zigzag leakage is short-circuited by one stator tooth; the second part links only part of the windings of a phase; the third part traveling from tooth to tooth does not link any coil. Although

the last two portions are well described in the literature [5], an analytical model for the first portion has not been found. In fact, the zigzag leakage flux short-circuited by one stator tooth has a dominant effect on PM machines, especially for the semi-closed slots. To model this part of the zigzag leakage flux will be the other emphasis of this paper.

The new models of the air gap and zigzag leakage fluxes are proven by FEM analyses to be an error of as low as 0.7% and 0.3%, respectively. The two models should be beneficial for designing and optimizing of machines.

II. ANALYTICAL MODEL OF AIRGAP LEAKAGE FLUX

A. Assumptions and Equivalent Circuit

The magnetic circuit approach is used to analyze the model machine with a simplified motor topology. This approach takes the leakage flux into account and yields analytical expressions for the average flux densities within the air gap and magnets.

Fig. 1 shows the motor topology as a linear translation equivalent, which is suitable for any specific topology. To simplify the problem, it is assumed that there is no saturation occurring in the steel regime, and the magnetic field intensity produced by the armature current in the stator windings is negligible. Given the flux distribution indicated in Fig. 1 and the Ohm's law equivalent for magnetic circuit, the equivalent magnetic circuit is presented and shown in Fig. 2 in which the variables are defined as:

- Φ_g air gap flux for one magnet pole
- Φ_r flux source of one magnet pole
- R_g reluctance corresponding to Φ_g
- R_{mo} reluctance of a magnet, corresponding to Φ_r
- R_s reluctance of the stator back iron
- R_r reluctance of the rotor back iron,
- R_{mr} reluctance caused by magnet-to-rotor leakage flux
- R_{mm} reluctance caused by magnet-to magnet leakage flux

By adding R_{mr} and R_{mm} in parallel with $2R_{mo}$, the equivalent circuit can take magnet-to-rotor and magnet-to magnet leakage flux effects into account.

Based upon the assumptions mentioned before, absence of saturation leads to negligible values of R_s and R_r with respect to R_g . Therefore, Fig. 2 can be reduced to Fig. 3, then to Fig. 4. In Fig. 4, R_m is calculated from Fig. 3 as

$$R_m = \frac{R_{mo}}{1+2\eta+4\lambda} \quad (1)$$

where

$$\eta = R_{mo} / R_{mr} \quad (2)$$

and

$$\lambda = R_{mo} / R_{mm} \quad (3)$$

B. Air Gap and Magnet Flux Densities

By flux division, the air gap flux can easily be obtained with

$$\Phi_g = \frac{R_m \Phi_r}{R_g + R_m} = \frac{\Phi_r}{1 + (R_g / R_{mo})(1+2\eta+4\lambda)} \quad (4)$$

Similarly, the flux leaving the magnet is obtained as

$$\Phi_m = \frac{1 + (R_g / R_{mo})(2\eta+4\lambda)}{1 + (R_g / R_{mo})(1+2\eta+4\lambda)} \Phi_r \quad (5)$$

Consequently, the flux densities within the air gap and the magnet are

$$B_{g,ave} = \frac{A_m / A_g}{1 + (R_g / R_{mo})(1+2\eta+4\lambda)} B_r \quad (6)$$

and

$$B_m = \frac{1 + (R_g / R_{mo})(2\eta+4\lambda)}{1 + (R_g / R_{mo})(1+2\eta+4\lambda)} B_r \quad (7)$$

where A_m / A_g is the ratio of the flux passing area of the magnet to that of the air gap.

The following expressions are easily obtained:

$$R_g = \frac{g_e}{\mu_0 (w_m + 2g_e)L} \quad (8)$$

$$R_{mo} = \frac{H_{PM}}{\mu_0 \mu_r A_m} \quad (9)$$

$$A_m = w_m L \quad (10)$$

$$A_f = w_f L \quad (11)$$

and

$$A_g = (w_m + w_f)L \quad (12)$$

where μ_0 is the permeability of air, L is the stack length of the laminated steel, and g_e is the effective width of the air gap taking into account the stator slotting. The fringing effect is also considered by adding the length $2g_e$ to w_m for the calculation of R_g .

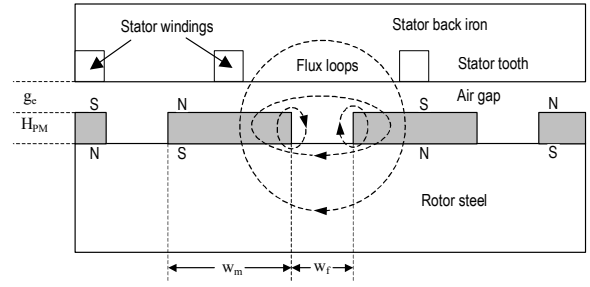


Figure 1. Simple linear translational motor topology

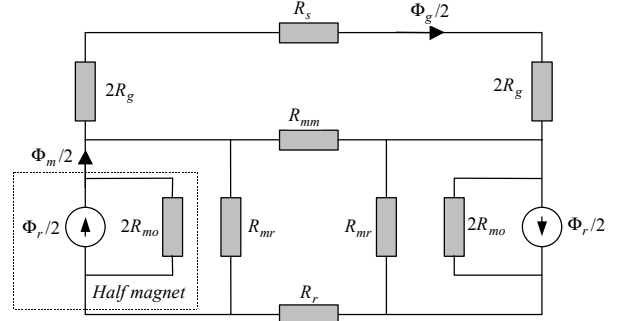


Figure 2. Equivalent magnetic lumped circuit for Fig. 1

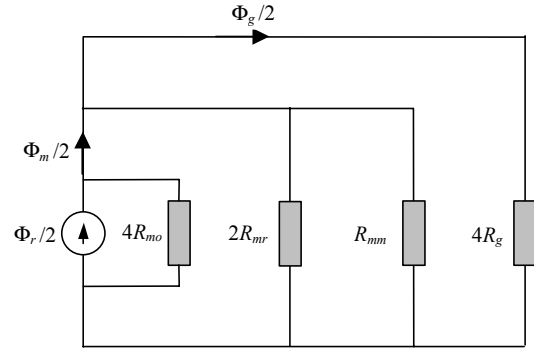


Figure 3. A reduced form of Fig. 2

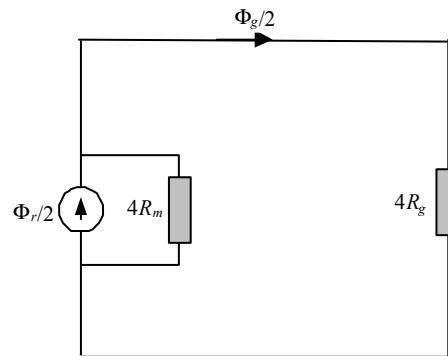


Figure 4. A reduced form of Fig. 3

C. Magnet-to-rotor and Magnet-to-magnet Reluctances

The expression of R_{mr} can be obtained by calculating its permeance. The circular-arc straight-line permeance model [6] is one of the most satisfactory techniques for modeling flux flowing in an air gap as depicted in Fig. 5 and 6. The fringing permeance P_{mr} is an infinite sum of differential width permeances, each of length $H_{pm} + \pi x$. That is

$$P_{mr} = \sum \frac{\mu_0 L dx}{H_{PM} + \pi x} \quad (13)$$

Because this equation involves differential elements, its solution for the case of $g_e < w_f/2$ is given by the integral

$$P_{mr} = \int_0^{g_e} \frac{\mu_0 L}{H_{PM} + \pi x} dx = \frac{\mu_0 L}{\pi} \ln\left(1 + \frac{\pi g_e}{H_{PM}}\right) \text{ for } g_e < w_f/2 \quad (14)$$

For the general case, P_{mr} can be expressed as

$$P_{mr} = \frac{\mu_0 L}{\pi} \ln\left[1 + \frac{\pi \min(g_e, w_f/2)}{H_{PM}}\right] \quad (15)$$

where $\min(\cdot)$ is the minimum function. Equation (14) will be used in this paper since $g_e < w_f/2$ is usually maintained.

Similarly, the permeance of magnet to magnet, P_{mm} , (refer to Fig. 6) is found as

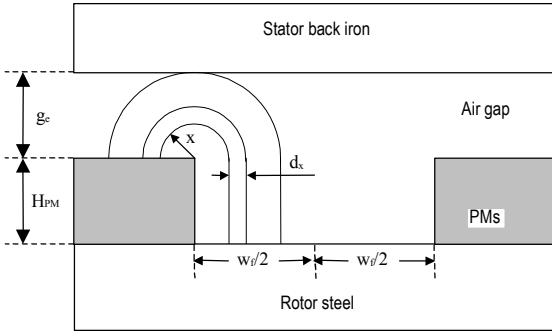


Figure 5. A circular-arc, straight-line permeance model of magnet-to-rotor leakage flux

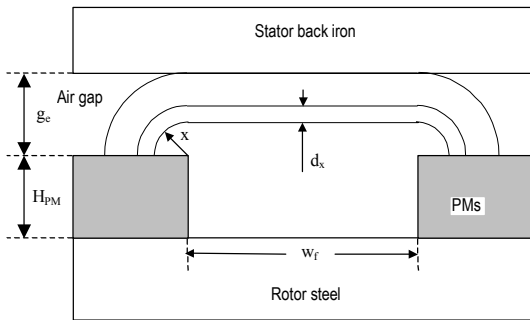


Figure 6. A circular-arc, straight-line permeance model of magnet-to-magnet leakage flux

$$P_{mm} = \frac{\mu_0 L}{\pi} \ln\left(1 + \frac{\pi g_e}{w_f}\right) \quad (16)$$

Using the above equations, and noting that the reciprocal relationship between reluctance and permeance depicted in (17) and (18),

$$R_{mr} = \frac{1}{P_{mr}} \quad (17)$$

$$R_{mm} = \frac{1}{P_{mm}} \quad (18)$$

(2) and (3) are transformed to (19) and (20), respectively.

$$\eta = \frac{H_{PM}}{\pi \mu_r w_m} \ln\left(1 + \frac{\pi g_e}{H_{PM}}\right) \quad (19)$$

$$\lambda = \frac{H_{PM}}{\pi \mu_r w_m} \ln\left(1 + \frac{\pi g_e}{w_f}\right) \quad (20)$$

D. Air Gap Leakage Flux Factor

Substituting (8) through (12) into (6) and (7), after some manipulation, yields

$$B_{g,ave} = \left[1 + \frac{w_f}{w_m} + \mu_r \frac{g_e}{H_{PM}} \frac{w_m + w_f}{w_m + 2g_e} (1 + 2\eta + 4\lambda)\right]^{-1} B_r \quad (21)$$

and

$$B_m = \frac{\left(1 + \frac{2g_e}{w_m}\right) \frac{1}{\mu_r} \frac{H_{PM}}{g_e} + 2\eta + 4\lambda}{\left(1 + \frac{2g_e}{w_m}\right) \frac{1}{\mu_r} \frac{H_{PM}}{g_e} + 1 + 2\eta + 4\lambda} B_r \quad (22)$$

At this point, it is convenient to analytically express the air gap leakage flux factor K_{Lg} in terms of the magnetic material properties and the machine dimensions. It is the ratio of the average air gap flux to that within the magnet, as depicted in (23), where η and λ are defined in (19) and (20), respectively.

$$K_{Lg} = \frac{\Phi_g}{\Phi_m} = \frac{1}{1 + \mu_r \frac{g_e}{H_{PM}} \frac{w_m}{w_m + 2g_e} (2\eta + 4\lambda)} \quad (23)$$

For design purposes the inverse forms of (21) and (22) are desired. That is, for a given $B_{g,ave}$ and B_r , the basic design quantity H_{PM} must be calculated. Unfortunately, these forms are not available because they are related to the solutions of the exponential equation $ye^y = C$, which has an infinite number of solutions y for each non-zero value of C . However, this process can be readily accomplished in computer by using an iteration to find the desired H_{PM} value (usually from 0 to 10 mm [5]) for the given $B_{g,ave}$ and B_r .

III. FEM VERIFICATION OF AIRGAP LEAKAGE FLUX MODEL

For numerical calculations, Table I gives the numerical data of the model motor shown in Fig. 1 and the analytical results calculated from (21) and (22). A few cases with the

different g_e 's, and w_f 's were investigated in order to evaluate the validity of (21) and (22). In addition, both ferrite magnet with $B_r=0.4$ Tesla and rare earth magnet with $B_r=1.07$ Tesla are employed in the FEM analyses. Table I shows that η associated with the magnet-to-rotor leakage flux has the same level effect on the total leakage flux as λ does. This result implies both the magnet-to-rotor and magnet-to-magnet leakage fluxes cannot be neglected, although the former is usually ignored in machine design.

For simplicity, the stator is considered to be slotless. Under this condition, a 2-dimensional magnetic analysis was conducted using the commercial finite element package Maxwell[®] developed by Ansoft Corporation. Table II shows the FEM results and the comparison between the analytical predictions and numerical calculations for the different B_r 's, g_e 's, and w_f 's. From Table II, note that the errors of $B_{g,ave}$, B_m , and K_{Lg} are all less than 1%, even for the extreme case (case 9), for which w_f is only twice of the air gap, even though it is usually not used in practice. This means that the analytical model has very high accuracy, and is valid and suitable for the purpose of design and optimization.

IV. ANALYTICAL MODEL OF ZIGZAG LEAKAGE FLUX

In addition to the air gap leakage flux discussed in the last section, zigzag leakage flux is another main part of the leakage flux.

TABLE I. THE ANALYTICAL RESULTS OF THE AIR GAP LEAKAGE FLUX

Case No.	Geometrical dimensions			Analytical results				
	g_e (mm)	w_f (mm)	B_r (T)	λ (10^{-2})	η (10^{-2})	B_m (T)	$B_{g,ave}$ (T)	K_{Lg}
1	0.5	5.0	0.40	1.675	2.031	0.3565	0.2815	0.9869
2	0.5	5.0	1.07	1.656	2.008	0.9525	0.7520	0.9869
3	0.5	4.0	0.40	2.031	2.031	0.3566	0.2927	0.9852
4	0.5	4.0	1.07	2.008	2.008	0.9527	0.7821	0.9852
5	1.0	5.0	0.40	2.989	3.554	0.3263	0.2498	0.9569
6	1.0	5.0	1.07	2.956	3.514	0.8711	0.6669	0.9569
7	1.0	4.0	0.40	3.554	3.554	0.3266	0.2591	0.9521
8	1.0	4.0	1.07	3.514	3.514	0.8719	0.6918	0.9521
9	1.0	2.0	0.40	5.725	3.514	0.3271	0.2776	0.9333

At $H_{PM} = 4.0$ mm, $w_m = 20.0$ mm, $\mu_r = 1.05/1.0384$ for $B_r = 0.40/1.07$, respectively.

TABLE II. THE FEM RESULTS AND THE ERRORS OF THE ANALYTICAL RESULTS

Case No.	FEM results			Error (%) [*]		
	B_m (T)	$B_{g,ave}$ (T)	K_{Lg}	B_m (T)	$B_{g,ave}$ (T)	K_{Lg}
1	0.3585	0.2824	0.9849	0.6681	0.3464	-0.2022
2	0.9553	0.7530	0.9853	0.2930	0.1349	-0.1586
3	0.3585	0.2925	0.9788	0.6714	-0.0950	-0.6495
4	0.9554	0.7798	0.9794	0.2845	-0.3023	-0.5885
5	0.3269	0.2502	0.9569	0.3864	0.1731	-0.0083
6	0.8705	0.6677	0.9588	-0.0665	0.1227	0.1890
7	0.3275	0.2581	0.9457	0.4598	-0.4148	-0.6724
8	0.8715	0.6911	0.9516	-0.0460	-0.1000	-0.0539
9	0.3299	0.2770	0.9236	0.7171	-0.2119	-0.9357

*: Error=(FEM results - Analytical results) / FEM results*100.

A. Zigzag Leakage Components and Assumptions

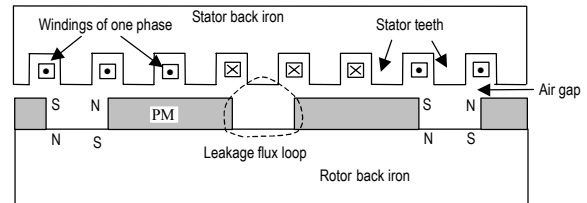
The zigzag leakage can be composed of three portions depicted in Fig. 7a through 7c. One part of the zigzag leakage depicted in Fig. 7a is what is short-circuited by one stator tooth. It has strong effect on PM machines, especially for the semi-closed slots depicted in Fig. 8. The zigzag leakage flux short-circuited by one stator tooth will be the emphasis of this section.

The zigzag leakage flux depicted in Fig. 7b links only part of the windings of a phase and the flux in Fig. 7c traveling from tooth to tooth does not link any coil. Both of two types of leakages are similar as those in induction machines and are well described in the literature [5].

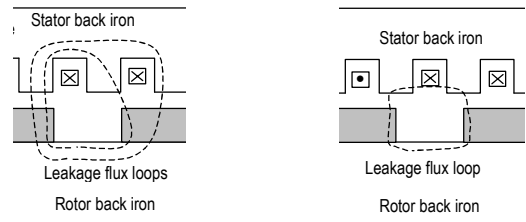
In order to obtain an analytical expression for the zigzag leakage flux in terms of the magnetic material properties and the machine dimensions, some assumptions are needed to simplify the problem: there is no flux saturation in the teeth or stator and rotor back iron, so that the reluctances associated with iron are negligible. Another assumption is that the half of the sum of the tooth width t_o and the opening b_o between any two adjacent teeth is larger than the distance w_f between two adjacent magnets (refer to Fig. 8). It is

$$\frac{t_o + b_o}{2} > w_f \quad (24)$$

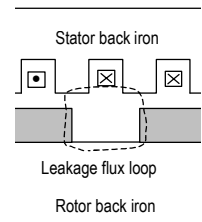
For normal machines, this condition is usually met and not a problem.



(a) leakage flux short-circuited by one tooth



(b) leakage flux linking a part of one phase winding



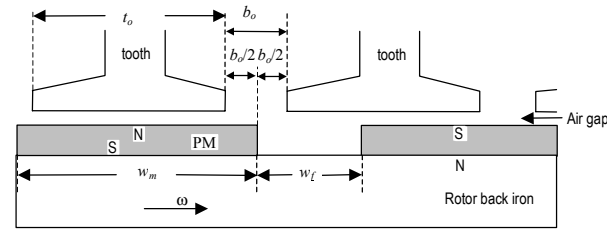
(c) leakage flux going through tooth to tooth

Figure 7. Zigzag leakage fluxes shown in the linear translational topology

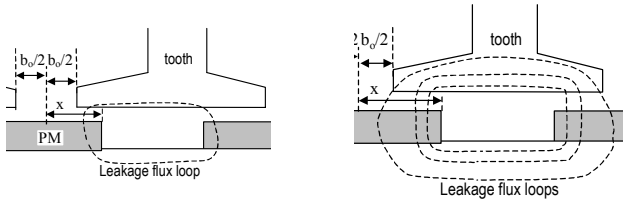
B. Analytical Model

Under the assumptions in section A, the zigzag leakage flux short-circuited by one stator tooth can be investigated by analyzing the flux distribution depicted in Fig. 8.

In Fig. 8, x is defined as the distance between the magnet right edge and the centerline of the tooth opening. It is convenient to define that the range of x is from 0 to $t_o + b_o$ with the period of $t_o + b_o$. From the flux shown in Fig. 8a through 8c, note that there is no leakage flux when $x=0$. The leakage flux Φ_{Lt} increases as x increases to its maximum value at $x=(b_o + t_o - w_f)/2$. The leakage flux will then decrease as x increases until $\Phi_{Lt} = 0$ at $x=b_o + t_o - w_f$ since the overlap portion between the tooth overlapping with the first magnet and the second magnet is becoming smaller. During $b_o + t_o - w_f < x < b_o + t_o$, Φ_{Lt} is almost negligible due to the slot opening present between the magnets. The maximum value of Φ_{Lt} can be found by flux division over the tooth width as



(a) no zigzag leakage at $x=0$



(b) Increasing leakage flux as x increases to $(t_o + b_o - w_f)/2$ from 0

(c) Maximum leakage flux at $x=(t_o + b_o - w_f)/2$

Figure 8. Illustrating calculation of zigzag leakage coefficient

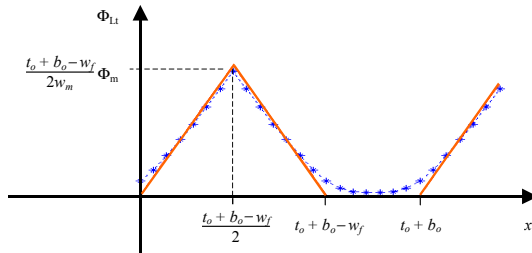


Figure 9. Approximate relationship between Φ_{Lt} and x

$$\Phi_{Lmax} = \frac{t_o + b_o - w_f}{2w_m} \Phi_m \quad (25)$$

where Φ_m is the flux leaving the magnet.

Further FEM investigations, discussed in the next section in detail, demonstrate that the relationship between Φ_{Lt} and x for $0 < x < b_o + t_o - w_f$ can be approximated as a straight line shown in Fig. 9. In Fig. 9, the dashed line with the marks “*”, which indicate the FEM measured points, shows the FEM results from the next section. Based upon this figure, the leakage flux Φ_{Lt} can be summarized as

$$\Phi_{Lt} = \begin{cases} \frac{\Phi_m}{w_m} x & \text{for } 0 < x < b_o + t_o - w_f \text{ and} \\ 0 & \text{for } b_o + t_o - w_f < x < b_o + t_o \end{cases} \quad (26)$$

The solid line in Fig. 9 shows the analytical result from (26). The leakage flux for $b_o + t_o - w_f < x < b_o + t_o$ shown in Fig. 9 is not exactly zero due to another type of zigzag leakage flux depicted in Fig. 7c, but is negligible compared with that short circuited by the teeth.

Given that the equation above is for one side of the leakage flux only, the average leakage flux for both sides of a magnet over one tooth pitch should be given by the integral

$$\Phi_{Ltave} = \frac{2}{t_o + b_o} \int_0^{t_o + b_o - w_f} \frac{\Phi_m}{w_m} x \, dx \quad (27)$$

The solution of this integral is

$$\Phi_{Ltave} = \frac{(t_o + b_o - w_f)^2}{w_m (t_o + b_o)} \Phi_m \quad (28)$$

Up to this point, the leakage flux coefficient K_{Lt} caused by the flux short-circuited by a tooth can be easily defined as

$$K_{Lt} = \frac{\Phi_{Ltave}}{\Phi_m} = \frac{(t_o + b_o - w_f)^2}{w_m (t_o + b_o)} \quad (29)$$

The airgap and zigzag leakage fluxes expressed by the factor K_{Lt} and K_{Lg} are two of the key factors in machine design and optimization to accurately predict the tooth flux density and the torque. In addition, the other leakage fluxes, such as slot, end-winding, and harmonic leakage fluxes, should also be properly considered.

V. FEM VERIFICATION OF ZIGZAG LEAKAGE FLUX MODEL

The FEM analysis will be given to verify the analytical equations in this section. The parameters used in the FEM model are $t_o=17$ mm, $b_o=3$ mm, $w_f=6$ mm, $w_m=48$ mm, $H_{PM}=6$ mm, $g=1$ mm, $\Phi_m=0.01644$ webers.

The results are shown in Fig. 9 and Table III, in which the distance x was defined in Fig. 8b and 8c. Fig. 10a through 10d demonstrate the change of the flux distribution as the rotor moves. From these figures, it is clear that the zigzag leakage flux is clearly a function of the relative position of the stator

tooth to rotor PMs. The minimum leakage flux is associated with Fig. 10a, in which the center lines of the slot opening and the magnet spacer are aligned, while the maximum leakage occurs when a tooth aligns with an interpolar space in Fig. 10d.

More specific digital results are shown in Table III. The ratio of the leakage flux at two magnet edges over the total magnet flux clearly shows the zigzag leakage can be as high as 27.8% of the total flux. Table III also shows that slotting has some effect on the total magnet flux, although it changes by a very small percent.

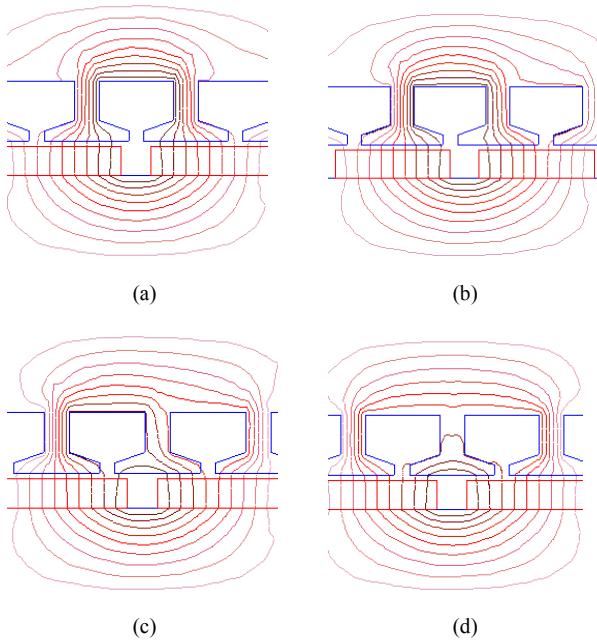


Figure10. Zigzag leakage fluxes short-circuited by a tooth
(a): the minimum leakage flux at $x = -3$ mm
(b): the increasing leakage flux as x increases ($x=0$ mm)
(c): the increasing leakage flux as x increases ($x=4$ mm)
(d): the maximum leakage flux at $x = 7$ mm

TABLE III. ZIGZAG LEAKAGE FLUXES FOR ONE OF TWO MAGNET EDGES

x (mm)	Zigzag Leakage flux Φ_L (wb)	Half of the total magnet flux Φ_m (wb)	$\frac{2\Phi_L}{\Phi_m} \times 100$
-3	5.1549E-5	0.0082231	0.63%
-2	6.5361E-5	0.0082213	0.80%
-1	0.000127077	0.0082125	1.55%
0	0.00026012	0.0082098	3.16%
1	0.000455832	0.0083983	5.55%
2	0.000723206	0.0082046	8.80%
3	0.00102889	0.0082102	12.52%
4	0.00130141	0.0082191	15.83%
5	0.00162805	0.0082265	19.81%
6	0.0019615	0.0082329	23.86%
7	0.00228365	0.0082339	27.78%

By evaluating (29), the average leakage flux for both magnet edges is found as 20.4%, while that result from FEM analysis is 21.2%. This implies that the error between them should be $20.4\% - 21.2\% = -0.8\%$. Obviously the error is dominated by the leakage flux going from tooth to tooth and is strongly dependant upon the slot opening and the flux density in the iron. Removing the leakage flux traveling from tooth to tooth which has not been modeled in (29), this number is reduced to $20.4\% - 20.7\% = -0.3\%$, which is the error of (29) for this case.

VI. APPLICATION TO A PM MACHINE

The analytical models of the air gap and zigzag leakage fluxes developed in the previous sections were used to optimize and design a completely new PM machine – Dual-rotor, Radial-flux, Toroidally-wound, Surface-mounted PM machine [7].

A 3-horsepower, 1800 RPM, 8-pole prototype machine was design and built with the designed output torque of 11.87 Newton-meter and efficiency of 87%. The experimental results of the prototype show that the output torque at the steady state is 11.78 Newton-meters and efficiency is 87.1%. Both values well match the design values. This type of correlation on a completely new machine concept implies that the flux distribution in the entire machine including air gap and zigzag leakage fluxes must be accurately predicted, as well as proving the validity of the two models.

VII. CONCLUSIONS

Analytical models for the airgap and zigzag leakage fluxes in a surface-mounted permanent magnet machine have been presented and proven by FEM analyses to yield accurate results. The two models should be beneficial for designing and optimizing of PM machines. More specifically, the following conclusions can be made:

The FEM analyses show that the two models have an error of as low as 0.7% and 0.3%, respectively, for the examples used in this paper.

Table I shows that the magnet-to-rotor leakage flux expressed by η has the same level effect on the total leakage flux as the magnet-to-magnet leakage fluxes expressed by λ does. That implies both the magnet-to-rotor and magnet-to-magnet leakage fluxes cannot be neglected, although the former is usually ignored in machine design.

Zigzag leakage flux encompasses a large portion in the total leakage fluxes and therefore will have a significant influence on the performance of PM machines with half-closed slots.

While not treated here, other leakage fluxes, such as slot, end-winding, and harmonic leakage fluxes, clearly should also be considered in a complete PM machine design.

REFERENCES

- [1] T. A. Lipo and Yue Li, "CFMs - A New Family of Electrical Machines", *IPEC '95*, Japan, April 3-7, 1995, pp. 1-8.
- [2] Y. F. Liao, F. Liang and T. A. Lipo, "A Novel Permanent Magnet Motor with Doubly Salient Structure", *IEEE-IAS Conf. Rec.*, 1992, Houston, TX, Vol. 1, pp. 308-316,

- [3] G. Jack, B. C. Mecrow, P. G. Dickinson, D. Stephenson, J. S. Burdess, J. N. Fawcett, and T. Evans, "Permanent Magnet Machines with Powdered Iron Cores and Pre-pressed Windings", *IEEE-IAS Conf. Rec.*, 1999, Phoenix, AZ, Vol.1, pp. 97-103.
- [4] W. Tsai, and T. Chang, "Analysis of Flux Leakage in a Brushless Permanent-Magnet Motor with Embedded Magnets", *IEEE Trans on MAG*, Vol.35, No.1, January 1999, pp. 543-547.
- [5] T. A. Lipo, *Introduction to AC Machine Design*, Wisconsin Power Electronics Research Center, University of Wisconsin-Madison. 1998.
- [6] D. C. Hanselman, *Brushless Permanent-Magnet Motor Design*, New York, McGraw-Hill, 1994.
- [7] R. Qu and T. A. Lipo, "Dual-rotor, radial-flux, toroidally-wound, permanent-magnet machines", *IEEE-IAS Conf. Rec.*, 2002, Pittsburgh, PA, Session 33, paper 5, in press.